Numerical simulation of Air-Water flow in bottom outlet

A. Shamsai[1], R. Soleymanzadeh[2]

[1]Prof ,Civil engineering department - Sharif University of Technology
Email: Shamsai@sharif.edu

[2]M.S student of civil engineering - Sharif University of Technology
Email: r_soleymanzadeh@yahoo.com

***Abstract:** Flow regime in dam's bottom outlet is divided in pressurized flow and free surface flow by the gate located for discharge control. Down stream tunnel involves high velocity Multi component Air –water flow studied by mathematical model. In this research work, we used Finite volume mixture two phase flow model. Because of high Reynolds number, standard two equations k-ε turbulence model was used. Model was verified by backward-facing step flow and results have been compared with experiments founded by Durst and Schmitt. Air demand ratio has been determined as function of Froude number at contracted section. Flow patterns have been compared at two categories of slug & stratified flows, Air mean concentration profile has been obtained at down stream tunnel. Comparison of flow pattern at two case with and without of aeration was investigated. Pressure drop behind of the gate and formation of vortex flow after the gate section have been discussed. Measurement of flow discharge and determination of contraction coefficient of the gate was outlined.*

***Keywords:** Two phase flow, Bottom outlet, CFD, Aeration, Cavitation*

Introduction

Bottom outlets convey high velocity Air-Water mixture flow. In large dams, they are commonly used for reservoir drawdown, sediment flushing, river diversion and environmental flow releases [1]. A typical example is a bottom outlet when a high-velocity supercritical air water flow discharges past from control gate (Fig. 4). Such high-velocity free-surface flows are extremely turbulent flows and flow Reynolds number is about $8*10^8$ [2]. Little research has been conducted systematically in the air-water flow properties of the high-velocity waters discharging at the downstream end of the tunnel [3]. Experimental studies of high-velocity water jets discharging into the atmosphere were often limited to visual observations [4]. Some researchers performed air concentration distribution measurements [5], but limited works

included air-water velocity and pressure distribution measurements [6].

This paper aims to provide some new understanding of the air-water flow properties in high-velocity water jets discharging past upstream pressurized and downstream free surface tunnel. New numerical investigations of two phase flow model were conducted systematically. The data are compared with experimental results. The results provide new insights into the interactions between the high-velocity water jet and the surrounding air.

At upstream of the gate, pressurized flow occurs, the gate might be vibrated because of high speed fluid and low pressure due to suction induced by high momentum fluid down stream of the gate [7]. Also large down

pull forces can be occurred. Common application to reduce suction and adverse effects of it, is aeration of the downstream face of the gate by means of ventilation shafts located immediately after the gate [8]. At design of ventilation shaft, the maximum air demand should be estimated. At steady state condition ,it is occurred at 50 to 80% gate opening [9]. Unsteady flow occurs when the gate starts closing. The maximum air discharge is observed near the complete closure at about 8 to 16% gate opening [8]. Appropriate dimensioning and determination of the pressure drop across the shaft allows estimation of the reduced pressure acting on downstream of the gate which is an essential parameter in the analysis of the structural components which must withstand the imposed loads. Pressure drop after gate section must be prevented from becoming too low as cavitation damage presented. Another problem at low pressure is water column separation for long time operation periods which cause water hammer [10]. Another consequence of low pressure is the large down pull forces that act under the gate [11]. There forces should be added to dead weight of the gate at design of hoisting device system. Down stream tunnel aeration prevents pressure drop and beginning cavitation. Air bubbles mix into water, Air-water compressibility reduces undesirable effect of water vapor bubbles collapsing [12]. Depend on air discharge to water discharge ratio and development of flow pattern, different categories of air water flow occur in down stream tunnel [3].

In this literature, the aerated water flow has been studied for the following reasons:

(1) The entrained air increases the bulk of the flow which must be taken into account when designing spillways and bottom outlets [3].
(2) The presence of air within the boundary layer reduces the friction drag and the resulting increase of momentum must be considered when designing a ski jump and/or stilling basin downstream of a bottom outlet [13].

(3) The presence of air in the high velocity flow may be prevent or reduce the cavitation erosion damage [5].

(4) The presence of air enhances the air-water transfer of atmosphere gases, e.g. nitrogen, oxygen, carbon dioxide [5]. Furthermore, it has been found that the entrained air dramatically enhances the compressibility of the flow.

At this research, two types of slug flow and stratified flow were investigated. Spray flow occurs at less than 20% of the gate opening status [3]. The gate slot and large air discharge versus water discharge lead to spray water at down stream tunnel. Steady state air demand has been subjected by Sharma [14], Garcia (1984), Falvay [3] and Speerli& Hager [1]. The complete researches were demonstrated by Falvay introduced unsteady numerical method in air demand computation by using of mass continuity and momentum equations. Naudascher investigation about down pull forces consequence, vibration of the gate and scale effect in the gates modeling are useful summaries at this session [15].

Flow pattern and hydraulic characteristics basically depend on the geometry of the bottom outlet and ratio of air discharge to water discharge [16]. Therefore, many engineers prefer using hydraulic models results at design of air vent and best hydraulic section at the gate section. Not only this method is time consuming and costly, but also the results depend on laboratory equipments, measurement devices accuracy

and geometry parameters modeling.

Simulation of free surface flows can be a useful tool both in the design of an industrial process or in exploring fundamental physical phenomena. At numerical modeling, dynamics of bubbles and droplets can be analyzed and it is possible to extract information from such simulations, which are very hard to obtain experimentally.

Unfortunately, very few papers on free surface flow modeling where two-phase flow model were adopted, have been published in the open literature. This is in contrast to the fact that most of the worldwide leading CFD vendors use these methods [17]. In this paper, we discuss the numerical model to solve the Navier Stokes equations for a multi-fluid situation. The technique is basically implicit and based on the PISO algorithm [18].

The paper demonstrates prediction of Air concentration at air-water mixture, Pressure drop after the gate, velocity profile and discharge measurements. In addition, the mixing of air in the water is considered. According to results of this investigation, it is possible to predict physical phenomena, which are hard to observe due to experimental limitations. Furthermore, Numerical results are in good agreement with experience.

Laboratory model

The experimental set-up may be subdivided into pumping station and approach conduit, gate chamber with a vertical gate, tailrace tunnel and return flow system. The total pump capacity was 360 L/s for approach heads up to 25 m. To improve the approach flow, the gate chamber was provided with flow strengtheners. The free surface down stream from the gate was smooth and non-aerated up to the inception point. The gate

was vertical and could be moved from the fully closed to the fully open position. This gate has not lip. The approach energy heads were 10, 20 and 30 m.

Downstream from the gate of height 0.30 m, the tailrace tunnel height increased under 45o to the tunnel height of 0.45 m. The tailrace tunnel had a width of 0.30 m and a maximum length of 21 m with a bottom slope of 2 %. Plexiglass covers made the tunnel air-proof. A rubber sheet was provided at the end of the air proof section to inhibit air access from the outlet.

The air supply conduit of 0.1 m diameter ran vertically into the up stream end of the tunnel where the height is increased. The air discharge in the ventilation conduit upstream from the end section was computed to within $\pm$ 2%. The air supply was controlled by orifice of throttling degrees ranging between 100 % (open) and 0% (closed). Air discharge was measured with a thermal probe located in the air supply pipe to $\pm$ 2%. Water discharge was measured by inductive discharge measurement upstream of the gate again to within + 2%. The mixture velocity in the tunnel flow was measured by VAW method. Local air concentration was measured by according for the electric conductivity between air and water by five probe located in parallel across the tunnel.

Numerical Model

Algebraic Slip Mixture Model Theory

The volume averaged continuity equation is :

$$\sum_{q=1}^{N} \alpha q = 1 \quad and$$

$$\frac{\partial}{\partial t}(\alpha_p \rho_p) + \frac{\partial}{\partial Xi}(\alpha_p \rho_p U_{m,i}) = -\frac{\partial}{\partial Xi}(\alpha_p \rho_p U_{Dp,i})$$

$$(1)$$

Table.1. Air and water volume fractions at boundaries

	α_{air}	α_{water}
Air vent enterance	1	0
Upstream inception point	0	1
Down stream end of the tunnel	1	0

No mass transfer is allowed in the algebraic slip mixture model. Therefore, right side of equation equals to zero [18].

The momentum equation for the mixture can be obtained by summing the individual momentum equations for both phases. It can be expressed:

$$\frac{\partial}{\partial t}\rho_{m,j}+\frac{\partial}{\partial Xi}(\rho_m U_{m,i} U_{m,j})=$$

$$-\frac{\partial P}{\partial Xi}+\frac{\partial}{\partial Xi}\mu_m\left(\frac{\partial U_{m,i}}{\partial Xj}+\frac{\partial U_{m,j}}{\partial Xi}\right)$$

$$+\rho_m\,g_j+Fj+\frac{\partial}{\partial Xi}\sum_{k=1}^{n}\alpha_k\rho_k\,U_{Dk,i}$$

$$\rho_m=\sum_{k=1}^{n}\alpha_k\rho_k$$

$$\mu_m=\sum_{k=1}^{n}\alpha_k\mu_k$$

$$\vec{U}_m=\sum_{k=1}^{n}\alpha_k\rho_k\vec{U}_k\Big/\rho_m$$

$$\vec{U}_{Dk}=\vec{U}_k-\vec{U}_m$$

$$(2)$$

Where n is the number of phases, ρ_m is the mixture density μ_m is the viscosity of the mixture and α is volume fraction.

In the present work, the energy equation has not been considered. Further, the experimental data used in the comparison were adiabatic. It has been assumed that no mass transfer between the phases takes place.

The algebraic slip mixture model differs from other multi phase flow models in two respects:

1- The algebraic slip mixture model does not assume that there is an interface between two immiscible phases; it allows the phases to be interpenetrating. The volume fractions α_q and α_p for a control volume can therefore be equal to any value between *0* and *1*, depending on the space occupied by phase *q* and phase *p*.

2- The algebraic slip mixture model allows the two phases to move at different velocities.
At this model volume fraction of each fluid should be known at boundaries. At air vent entrance, $\alpha=1$ and at upstream tunnel entrance $\alpha=0$ for air phase. This means that no air entrainment was assumed of upstream tunnel.

Discretization Scheme

In this research, the flow is not aligned with the grids, however, first-order convective discretization increases the numerical diffusion error. We were generally obtained more accurate results by using the second-order discretization. Furthermore, we used segregated solver for overall analysis.

For pressure interpolation, which calculations involving body forces, the

Implicit Body Force treatment was used for the body force formulation in the Multiphase Model. This treatment improves solution convergence by accounting for the partial equilibrium of the pressure gradient and body forces in the momentum equations [18].

The Pressure-Velocity Coupling Method

The PISO algorithm with neighbor correction was used for all transient flow calculations because it allows to use a larger time step, as well as an under-relaxation factor of 1.0 for both momentum and pressure. PISO with skewness correction was used for both steady-state and transient calculations on meshes with a high degree of distortion.

In this method, under-relaxation factors of 1.0 or near 1.0 are recommended for all equations. We used the PISO skewness correction for highly-distorted meshes, further, we set the under-relaxation factors for momentum and pressure so that they sum to 1 (0.3 for pressure and 0.7 for momentum).

Turbulence Modeling

The simplest of turbulence models are two-equation models in which the solution of two separate transport equations allow the turbulent velocity and length scales to be independently determined [19]. The standard k-ε model in FLUENT falls within this class of turbulence model and has become the workhorse of practical engineering flow

calculations in the time since it was proposed by Jones and Launder [18]. Robustness, economy, and reasonable accuracy for a wide range of turbulent flows explain its popularity in industrial flow and heat transfer simulations. It is a semi-empirical model, and the derivation of the model equations relies on phenomenological considerations and empiricism.

The turbulent kinetic energy, k, and its rate of dissipation, ε, are obtained from the following transport equations:

$$\rho \frac{Dk}{Dt} = \frac{\partial}{\partial Xi}\left[\left(\mu + \frac{\mu_t}{\sigma_k}\right)\frac{\partial k}{\partial Xi}\right] + G_k + G_b - \rho\varepsilon - Y_M$$

(3)

$$\rho \frac{D\varepsilon}{Dt} = \frac{\partial}{\partial Xi}\left[\left(\mu + \frac{\mu_t}{\sigma_\varepsilon}\right)\frac{\partial \varepsilon}{\partial Xi}\right]$$
$$+ C_{1\varepsilon}\frac{\varepsilon}{k}(G_k + C_{3\varepsilon}G_b) - C_{2\varepsilon}\rho\frac{\varepsilon^2}{k}$$

(4)

In these equations, G_k represents the generation of turbulent kinetic energy due to the mean velocity gradients, G_b is the generation of turbulent kinetic energy due to buoyancy, Y_M represents the contribution of the fluctuating dilatation in compressible turbulence to the overall dissipation rate, $C_{1\varepsilon}$, $C_{2\varepsilon}$ and $C_{3\varepsilon}$ are constants. σ_k and σ_ε are the turbulent Prandtl numbers for σ_k and σ_ε, respectively. We use following constants:

Table.2. The standard k-ε turbulence model constants

σ_ε	σ_k	C_μ	C_2	C_1
1.3	1.0	0.09	1.92	1.44

Numerical model verification

In this section the mixture two phase flow model which was discussed at preceding section, is verified. The accuracy of model is investigated using latest experimental and field data results.

Flow over backward-facing step

To compare the results of the CFD model with the experimental research work [20], a computational model has been created with 2-D element at Gambit software [21]. A finite volume map shape mesh has been used to model a backward facing step and result have been compared to the experimental presented in reference [20]. The flow with the Re=108600 is passing over a step with the height of H and the length of 5H and the tailrace of 20H. Fig.1 and Fig.2 show the stream function and pressure contours while Fig.3 shows comparison between velocity magnitudes of the CFD model results versus experimental respectively.
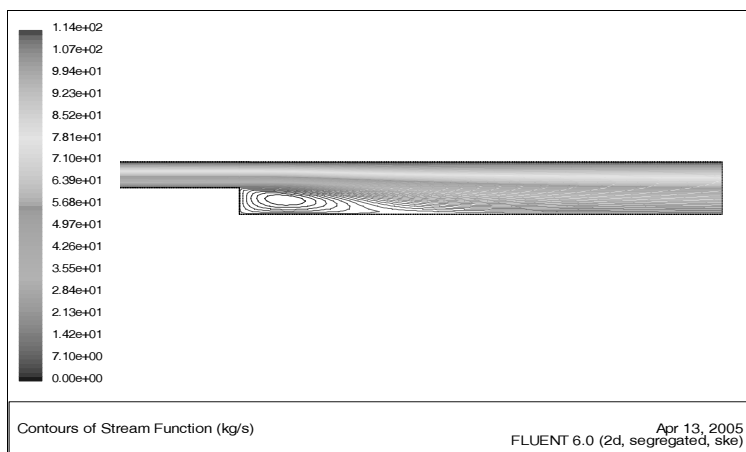

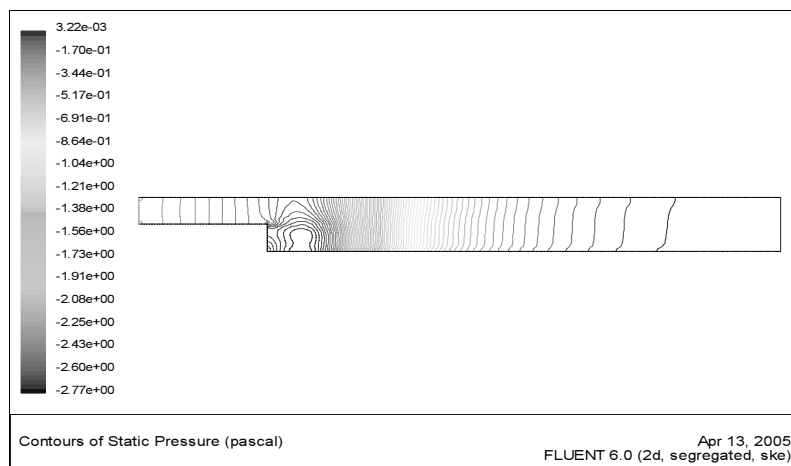**Fig.1.** Stream function and reattachment length prediction for the CFD model for step flow

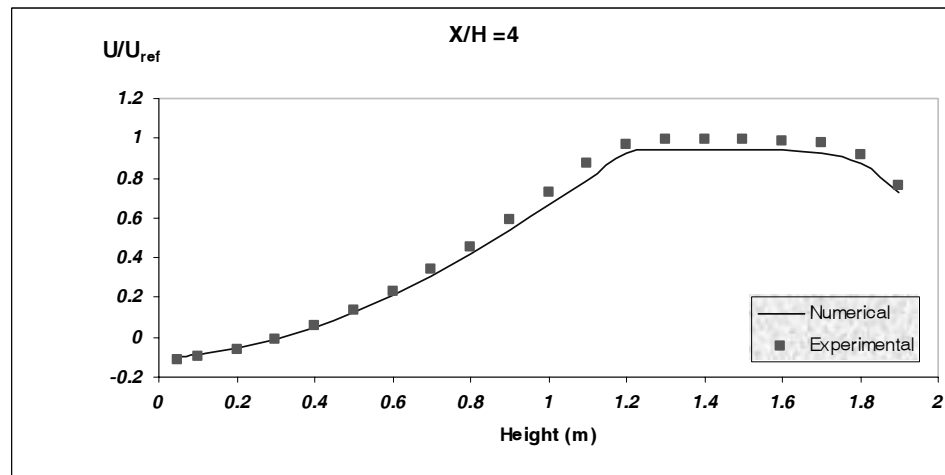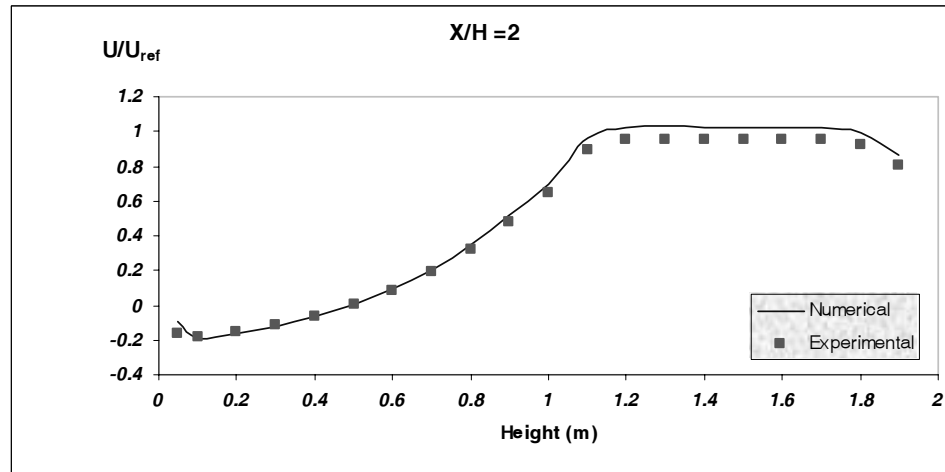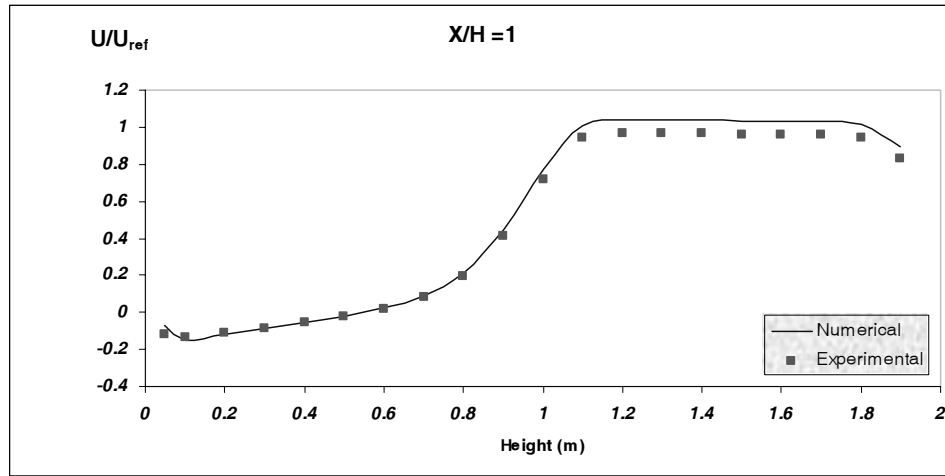**Fig.2.** Pressure contour for the CFD model for step flow

Fig.3. Normalized velocity profile for the CFD model versus the experimental data
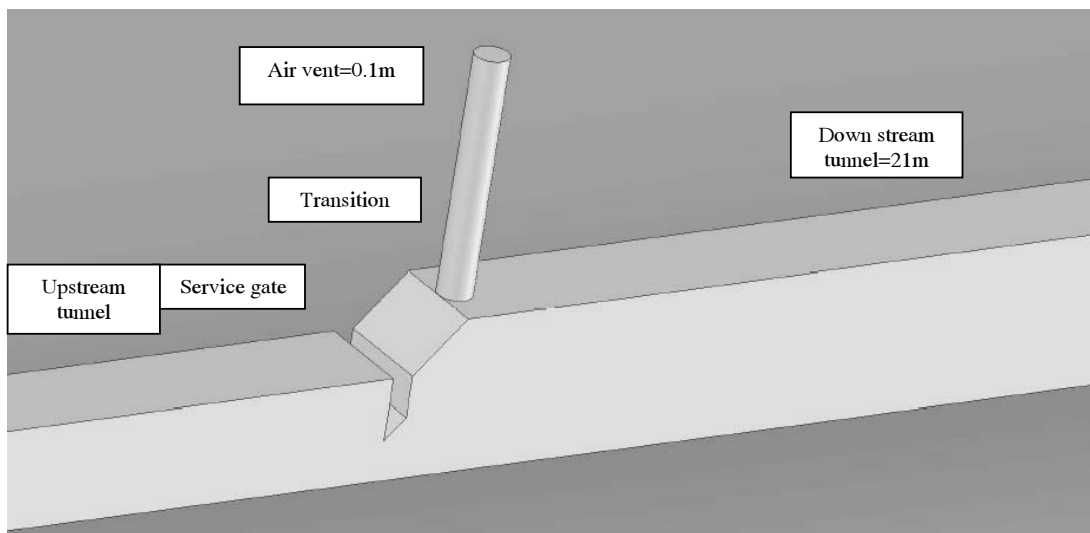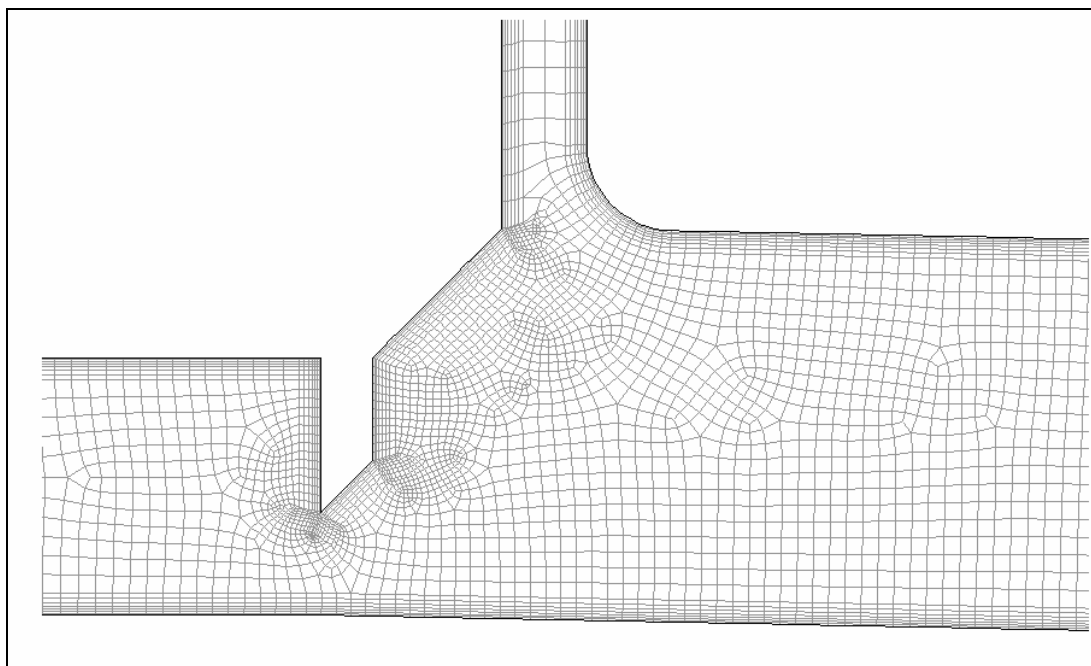
Fig.4. geometry of bottom outlet [1]

Fig. 5. Sample mesh for H=30 m, gate opening=40%

Parameter X in Fig.3 is horizontal distance between the velocity profile section and the Step. All dynamic velocities are normalized with respect to approach velocity (U=0.109 m/s) and the sectional geometry are normalized with respect to H. Comparison of results shows 5 and 6 percent error at determination of the velocity profile and the reattachment length respectively (Fig.1,3). Again it is appears from the results, there is a good agreement between the results in general.

Numerical model set up

It was assumed that both fluids (air and water) are incompressible. The advantage with this form is that the treatment of the density is now restricted to the stress and capillary terms.

We often run at courant number equal to 0.25 in which case, we only need less than 50 iterations per time step. However, in the case of convergence problems, we might increase the number of iterations per time step and under relaxation could be introduced.

Figure.4 shows the geometry of bottom outlet created at Gambit software where it has been analyzed at several gate opening and different approach head with the fluent mixture two phase flow model. It consists of approach tunnel, gate chamber, 45° transition, air vent and down stream tunnel.

L: Down stream tunnel length =21m
b: Width of upstream and downstream tunnel = 0.3m
D_1: Height of upstream tunnel =0.3m
D_2: Height of downstream tunnel =0.45m
d : Air vent conduit diameter=0.1m
S : Tunnel bottom slope =2%
Two bottom outlet structures were considered, bottom outlet with ventilation shaft and without it. Generally, a set of computational fluid dynamic analyses were performed by finite volume method. Our final goals were to obtain velocity and pressure distribution at flow field and other hydraulic parameters that are important to improve of bottom outlet designing.

CFD analyses were investigated by using three magnitudes of approach head 10-20 and 30 m and seven gate opening status 6.7-13.3-20-30-40-80% and 100%. At near wall, we used standard wall function formulation for velocity profile calculation. Therefore, the thickness of the first row meshes calculated regard to $y^+>30$. The sample mesh has been shown at Figure.5.

In this research work, the following simplifications were introduced.

1- Viscous and surface tension effects can be ignored [1]

$$(5)$$

$$Wb = \frac{\rho v^2 l}{\sigma} \rightarrow \textit{In this research ....Wb} > 110$$

$$\text{Re} = \frac{\rho v\, l}{\mu} \rightarrow \textit{In this research ....Re} > 10^5$$

Where, ρ is fluid density (kg/m^3), V is flow mean velocity (m/s), L is length (m), μ is dynamic viscosity (kg. m/s), σ is surface tension (N/m).

2- No mass transfer is allowed between air and water phases.

3 - The drag and the added mass force mainly undertake the interfacial momentum transfer. Effects of other forces between the two phases are negligible [10].

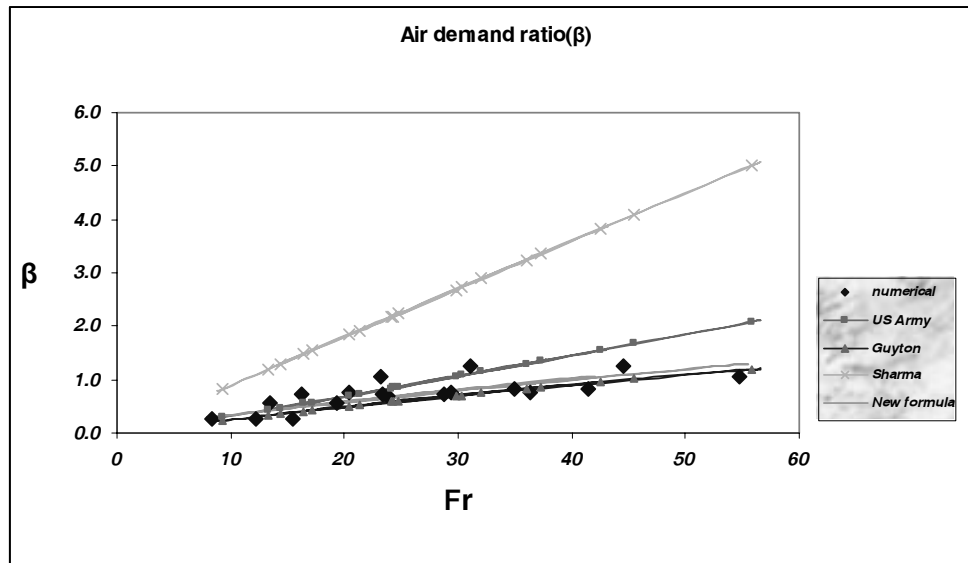**4-** Roughness is constant at conduit.

Fig .6 . Air demand ratio and comparison with Sharma , Guyton ,US army experimental relations

5-Mach number is always less than 0.3. Therefore, air can be assumed as incompressible fluid [10].

Results

Air demand ratio

Under certain conditions of operation, the pressure in a conduit may fall considerably below atmospheric pressure. Large reductions in these pressure fluctuations can be effected by providing air vents through which air will flow into the conduit where less than atmospheric pressure exists. The vents usually open through the conduit roof immediately downstream from the service gate. Air requirements are most critical in this area.

It is essential to introduce air at low-pressure areas to partly alleviate negative pressure conditions and to provide, air bubbles in the flow that will reduce the formation of

cavitation pockets and cushion the effects of their collapse. Determination of air demand ratio,,is important for design of air vent.

$$\beta = \frac{Q_{air}}{Q_{water}}$$

Where Q_{air} represents air demand discharge and Q_{water} represents water discharge. We calculated air demand ratio by CFD analyses and compared with experimental relations represented by Sharma, Guyton and Campbell and US army corps of engineering (Fig.6).

Following relation has been interloped from numerical results:

$$\beta = 0.0555 \times (Fr_c - 1)^{0.7869} \tag{6}$$

$$Fr_c = \frac{V}{\sqrt{g.Y_c}} , \quad V = \frac{Q}{b_c.Y_c}$$

Where Fr_c is Froude number, V is mean velocity, Y_c is flow depth at contracted

Table.3. Numerical error at calculation of air demand ratio, β.

Gate opening%	Fr Number	β Numerical (Qa/Qw)	β geiton	Numerical error %	β us army	Numerical error %
6.7	55.7	1.04	1.20	-15.2	2.09	-50.1
6.7	45.5	1.25	1.01	19.5	1.67	-25.4
13.3	42.5	0.81	0.95	-17.4	1.55	-48.0
20	37.3	0.75	0.85	-12.7	1.35	-44.4
13.3	36.0	0.82	0.82	0.1	1.30	-36.7
6.7	32.1	1.26	0.74	41.0	1.15	9.8
20	30.4	0.75	0.71	5.4	1.08	-30.7
30	29.8	0.72	0.70	2.7	1.06	-32.4
40	24.8	0.70	0.59	16.0	0.86	-18.4
30	24.3	0.74	0.58	21.2	0.85	-12.7
13	24.2	1.07	0.58	45.7	0.84	26.9
20	21.4	0.74	0.52	30.4	0.73	1.7
40	20.3	0.55	0.50	10.1	0.69	-20.4
80	16.4	0.27	0.41	-52.1	0.54	-50.6
30	17.2	0.72	0.43	41.0	0.57	25.9
40	14.4	0.56	0.36	34.9	0.47	18.8
80	13.2	0.26	0.34	-27.3	0.43	-38.1
80	9.3	0.27	0.24	8.7	0.28	-6.4
	Numerical Mean Error			8.4		-18.4

section, b_c is tunnel width and g is gravitational acceleration.

The air discharge and water discharge were calculated from numerical results and Y_c, depth, has been measured from the tunnel invert to water surface which air concentration is 99 percent.

Accuracy of numerical results demonstrated in Table.3. It exhibits 9 % error versus Guyton &Campbell and 18% error versus US army relations.

Cavitation

Cavitation results from the sudden reduction of local pressure at any point to the vapor pressure of water. Such reductions in pressure are caused in water passages by abrupt changes in the boundary. The partial gate operations cause a tendency of separation of the flow from the boundary

where produces high velocities and low pressures.

Vapor cavities form as bubbles in the low-pressure areas and collapse when a higher pressure area is reached a short distance downstream of the gate. The collapse is very rapid and sets up high-pressure shock waves or possibly small, high-velocity local "jets" in the water that cause damage to steel lining. The basic equation associated with cavitation studies is

$$\sigma = \frac{P - P_v}{\rho u^2 / 2} \tag{7}$$

Where, P is absolute pressure, P_v is water vapor pressure and u is flow mean velocity.

For all reservoir heads and gate openings, bottom slope is always greater than critical slope ($S > S_{critical}$). When the air vent wasn't designed or head loss at ventilation shaft is large that air negative pressure at ventilation

shaft is less than -1.5 m of water [1], air discharge through ventilation shaft isn't enough and aeration procedure is disturbed. Consequently, water fills the down stream tunnel and large recirculation takes place right after gate section. At constant gate opening, the length of vortex flow increases with increasing reservoir head (Fig.11). Slug flow forms and oscillatory waves occur at water surface. The pressure drops rapidly after the gate section.

Where boundary changes are abrupt or the local flow is highly turbulent, such as at gate slots, minimum cavitations index should not be lower than 0.2-0.25 for safe design. These values are based on experience and should be conservative [3].

We calculated velocity and pressure at the conduit by using numerical analyses. Cavitation index was calculated at two cases of construction (with air vent and with out of air vent) Fig.7 represents the comparison of cavitation index at two cases of aerated and not aerated flows. This demonstrates when velocity magnitude is greater than 20 m/s, cavitation index is less than critical range and aeration is necessary.

Air concentration at two phase flow

Air is naturally suctioned through ventilation shaft due to negative pressure after the gate section and mixes with water flow. Air bubbles penetrate into water due to vertical velocity and water surface turbulence. Air-water Mixing procedure starts near the gate section and continues toward the contracted section (Fig 8).

It is engineering concern calculating air concentration profile in two axial and transverse directions of two phase flow. We used mixture two phase flow model which

allows air bubbles to penetrate into water. Therefore, mixing procedure can be investigated. It is possible to calculate air concentration at any point by CFD analyses that acting of it is very difficult experimentally. In this section, we calculated decay of streamwise mean air concentration profile at three approach heads;10-20 and 30 m by CFD analyses and compared with experimental concentration data measured by accounting for the difference in electric conductivity between air and water.

For the present bottom outlet with a bottom slope of 2%, the mixture flow depth always increases. Accordingly After contracted section, the mixture depth starts growing to finally attain uniform flow depth. Because of buoyancy force, air bubbles releases from mixture. The present tunnel length was too short for complete air detrainment, wherein uniform pure water flow would exist sufficiently down stream from the gate [3]. Mean air concentration can be determined by following equations:

$$\hat{C} = \int_0^y c \cdot v \cdot dy \ / \ \int_0^y v \cdot dy \qquad (8)$$

$$X^* = \frac{x}{L} \qquad (9)$$

Where $\hat{C}$ is the air mean concentration at cross section, c is locally concentration, v is mean velocity, x is axial distance measured from the gate section and L is tunnel length measured from gate section. This integral was solved numerically and the results have been demonstrated at Fig.9.

The results exhibit that, maximum air concentration appears around contracted section and decrease toward tunnel outlet. With increasing the gate opening and the
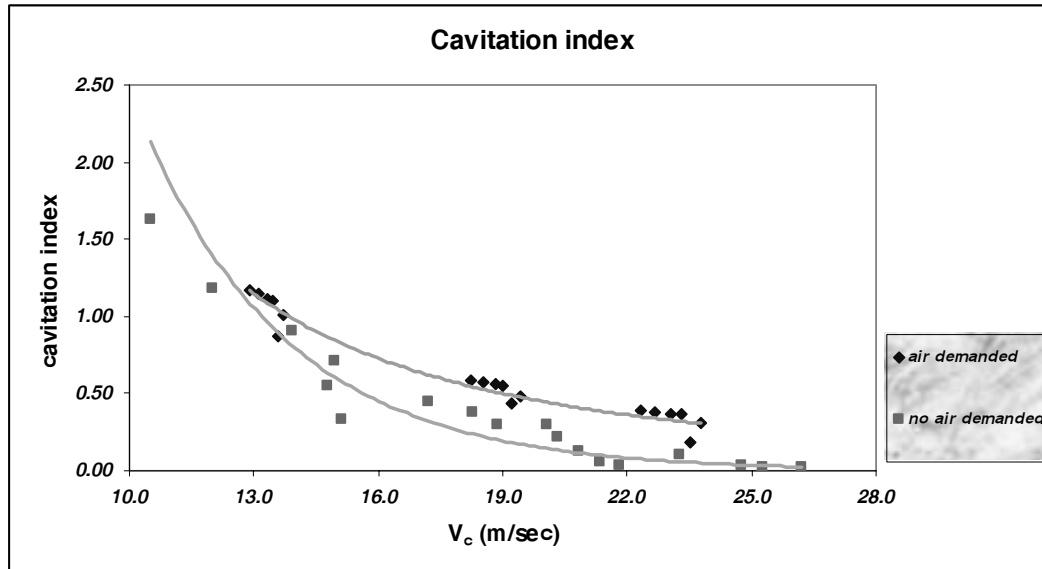
Figure.7.Comparison two case of air demanded air no air demanded at cavitation index for 10-20-30 m head and 6.7 ,13.3 ,20,30,40 percent gate opening
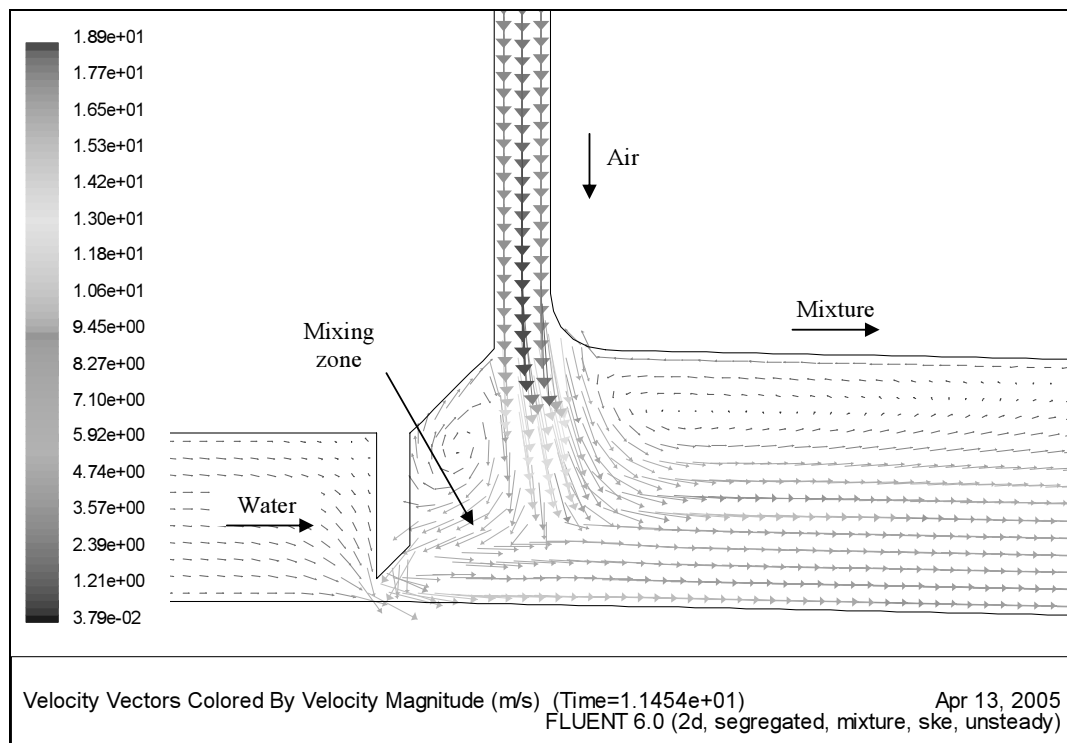

Velocity Vectors Colored By Velocity Magnitude (m/s) (Time=1.1454e+01)   Apr 13, 2005
FLUENT 6.0 (2d, segregated, mixture, ske, unsteady)

Fig.8. Vertical velocity vector and air bubbles penetration into water, H=10 m ,gate opening =13.3 %

H=10 m

Ĉ vs X*

Legend: 6.70%, 13.30%, 20%, 30%, 40%, 6.70%, 13.30%, 20%, 30%, 40%

Experimental (dashed), Numerical (solid)

H=20 m

Ĉ vs X*

Legend: 6.70%, 13.30%, 20%, 30%, 40%, 6.70%, 13.30%, 20%, 30%, 40%

Experimental (dashed), Numerical (solid)

H=30 m

Ĉ vs X*

Legend: 6.7, 13.3, 20, 30, 40, 6.7, 13.3, 20, 30, 40

Experimental (dashed), Numerical (solid)
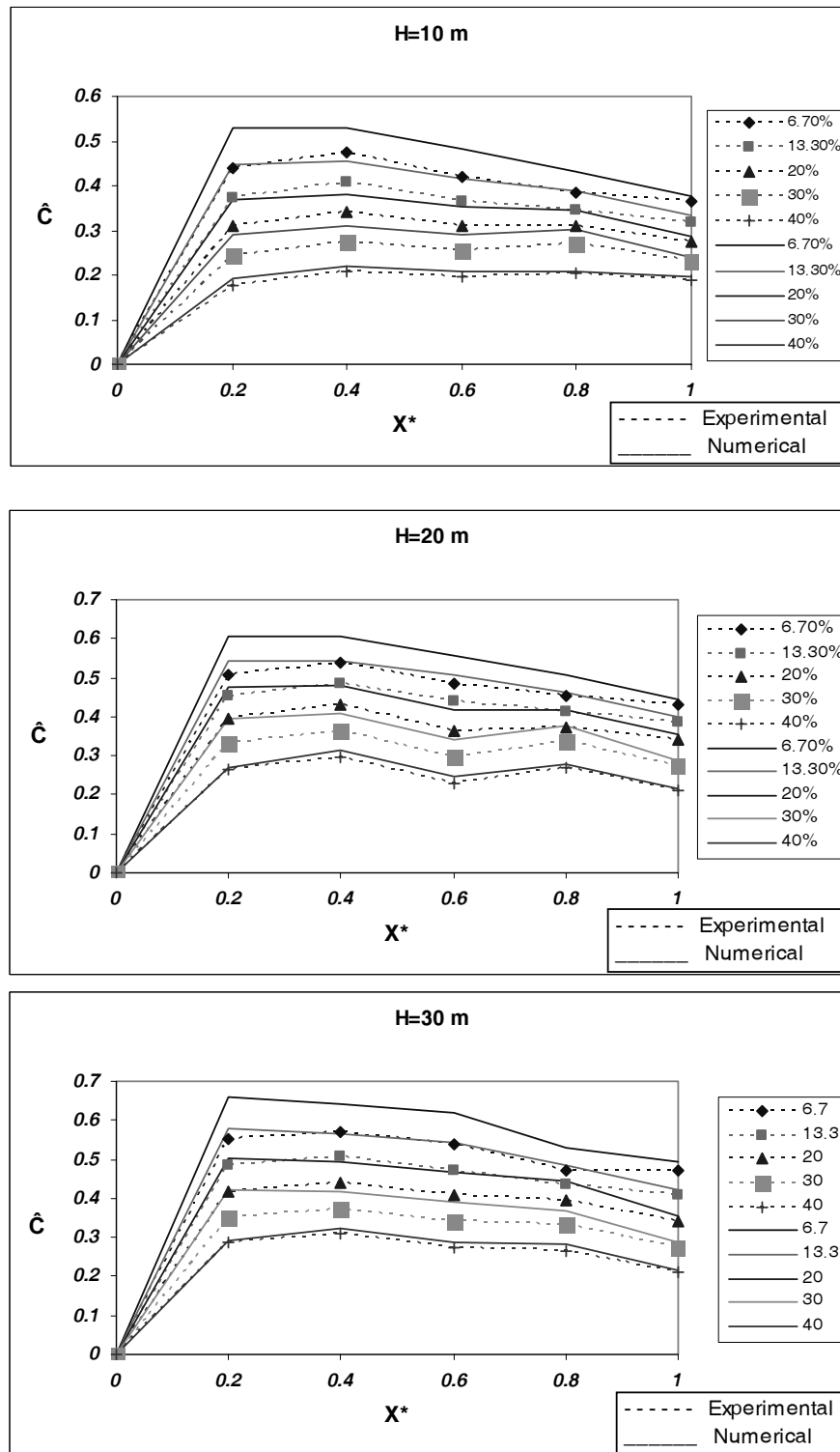
Fig.9.Decay of air mean concentration toward tunnel outlet for H=10,20,30 m and 6.7,13.3,20,30,40 %gate opening

reservoir head, the air discharge of ventilation shaft is increased. Mixing air and water increases mixture depth. The rate of depth increasing is larger near gate section and becomes smaller toward tunnel outlet. This situation take place because of mixing air and water near the gate section and detrainment of the air bubbles toward tunnel outlet because of deceleration. After gate section, free surface flow occurs and limited air section produces above the two phase flow. Air passes through this section because of shear stress between two phases [3].

In addition, axial air concentration was determined at the four cross sections A, B, C and D. Figure.10 shows axial air concentration distribution at two phase flow depth for several gate opening. It is close to zero near the tunnel invert and increase in S shape towards the mixture surface.

In the Fig.10, $Z_g = \dfrac{z}{h_{99}}$ where Z is vertical coordinate, is measured from tunnel invert, h_{99} is mixture depth with 99 percent air concentration, A=5, B=8, C=12 and D=16 m are distances which measured from gate section. According to the results, the quantity of experimental and CFD air volume fractions at tunnel invert and near water surface differs 25 percent and 10 percent, respectively. These differences caused by experimental measurement accuracy and 2-D CFD analyses. At 2-D analyses, it is impossible to consider secondary flow that affects mixing of air in water depth.

Discharge measurement

Down stream controlled flow

At closed conduits, flow discharge is controlled from downstream when conduit outlet is submerged. This situation should be avoided at bottom outlet, since it causes

formation of submerged hydraulic jump at tunnel and flow chocking. Air entrainment process is disturbed and low pressure occurs at down stream tunnel, the gate starts vibration. Fig.11 shows the formation of slug flow and oscillatory waves occurred because of no aeration at down stream tunnel.

Upstream controlled flow

In this paper, tunnel bottom slope is always greater than critical slope ($S > S_{critical}$) and there is not any restriction against air entrainment from ventilation shaft. Stratified flow was developed and flow discharge is controlled from the gate section. Discharge can be calculated by following empirical equations [1], [8]:

$$Q_g = A_g . C_d \sqrt{2g(H_1 - h_2 - \Delta h_g)}$$

$$(10)$$

$$C_d = \left(K_g + K_e y^2 + \frac{1}{C_c^{\,2}} \frac{V^2}{2g} \right)^{-0.5}$$

$$(11)$$

Where A_g is cross section under gate (m²), C_d is discharge coefficient, H_1 is reservoir head (m), h_c is water depth at contracted section (m), Δh_g is gate head loss (m), k_g is gate head loss coefficient, k_e is entrance head loss coefficient, C_c is contraction coefficient. e is gate opening and e_0 is tunnel height.

At first C_c should be determined, which strongly depends on locally flow condition at the gate section and the gate geometry [22].

$$h_c = C_c \times y \quad , \quad y = \frac{e}{e_0}$$

the contraction coefficient C_c has been determined at 6.7, 13.3, 20, 30, 40, 80, 100% of the gate opening. hc depth has been determined from numerical results.
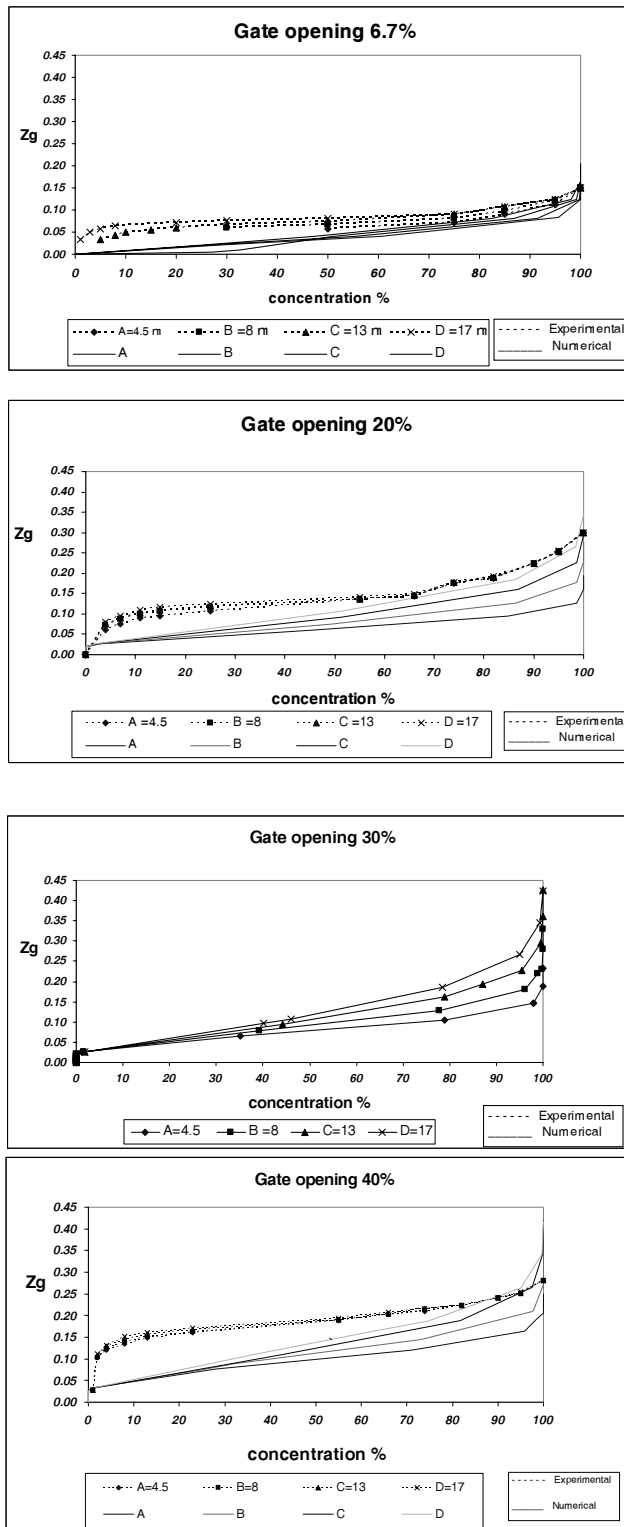
Fig .10. Axial air concentration distribution at distances A= 5m, B= 8m, C= 14m and D= 17 m from gate section, H1=10 m
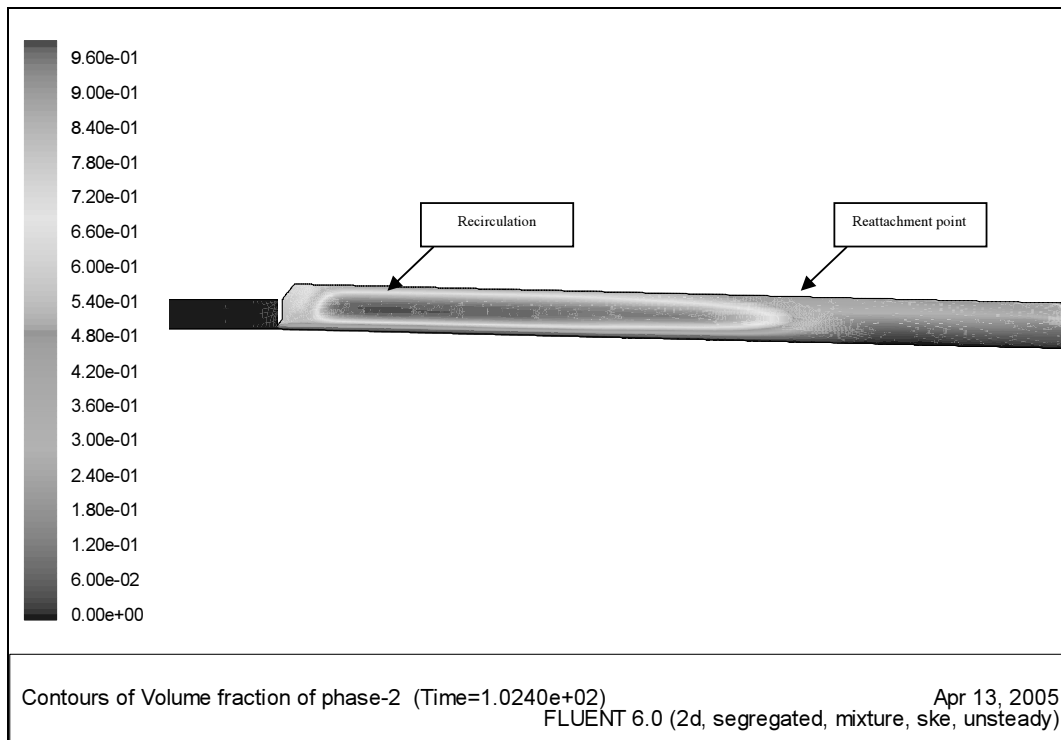
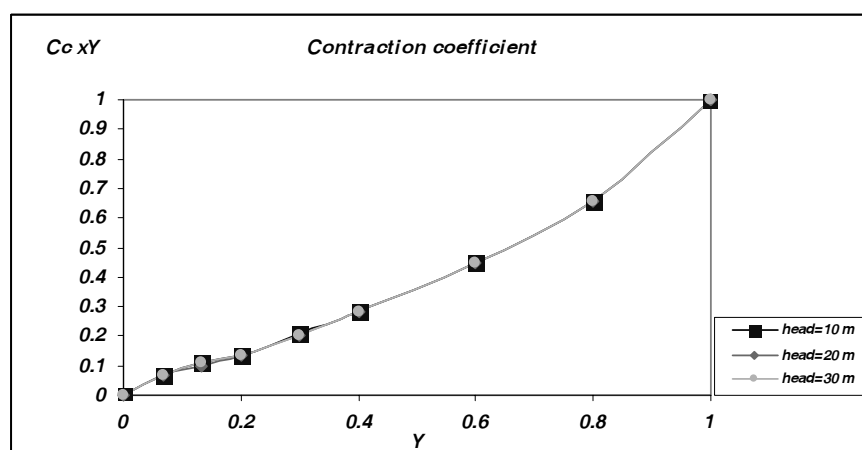**Fig.11.** Formation of slug flow, oscillatory waves and tunnel chocking for H=30 m, gate opening =13.3 %

Fig.12. Contraction coefficient at several gate opening and reservoir head
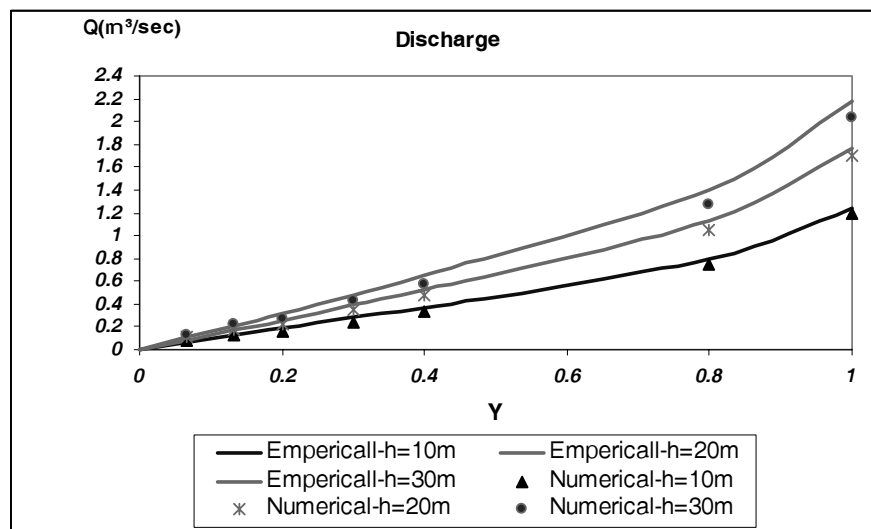
Fig.13. Comparison between numerical and experimental discharge, lines represent physical and points represent numerical data

Fig.12 shows C_c for three approach head, 10-20-30 m. It is founded that contraction coefficient is independent of reservoir heads and obeys only the gate opening.

Water discharge had been measured by inductive discharge measurement upstream of the gate to within $\pm$ 2%. It is possible to calculate flow discharge by CFD analyses. We found that measured discharge from laboratory model and numerical model are simultaneously and numerical method showed 3% error at discharge calculation (Fig 13).

CONCLUSION

Numerical simulation of two phase flow at bottom outlet at 6.7, 13.3, 20, 30, 40, 80 and 100 percent of the gate opening and 10-20 and 30 m approach head at two cases of aerated and not aerated flow conditions were investigated.

1- Air demand ratio at different status of gate opening and reservoir heads was determined as function of Froude number at contracted section according to formula (6). It has been compared with experimental relations. This comparison shows 9% difference with Guyton and 18% difference with US army relations according to table.3.

2- For the water velocity magnitude greater than 20 m/s, the cavitation index is less than critical range for closed conduit. Therefore, the down stream face of the gate should be aerated.

3- Comparison between experimental and numerical results at flow discharge measurement shows 3 % difference.

4- Decay of Air mean concentration towards the tunnel outlet was calculated and compared with experiment. The comparison shows 12 percent difference with experimental data. It starts to decrease from

the contracted section towards the tunnel outlet. Furthermore, maximum concentration appears around contracted section.

5- The axial air distribution at two phase flow depth at A, B, C and D sections measured from the gate section, has been determined, because of 2-D analyses and neglecting of secondary flow, comparison of experimental and numerical quantities shows 25 % and 6% difference at the tunnel invert and the water surface, respectively.

6- With convenient boundary conditions and modeling of closed conduit geometry, fluent results are trustable at modeling of two phase flow fields.

Notations

A : Cross-sectional area
A_c : Cross-sectional area at the vena contracta
A_g : Cross-sectional area at the gate section
C_c : Contraction coefficient
C_d : Discharge coefficient
e : Gate opening
Fr_c : Foude number at the vena contracta
g : Gravitational acceleration
H_1 : Reservoir water surface elevation
K_e : Local loss coefficientat the entrance
K_g : Local loss coefficient at the gate section
Q : Discharge
Q_a : Air demand
Q_w : Water discharge
U_s : Average velocity in the ventilation shaft
B : Tunnel width
x : Longitudinal distance
y : Dimensionless gate opening (e/e0)
ρ_a : Density of air
ρ_w : Density of water
R_g : Reynolds number at the gate section
U : Average velocity
U_c : Average velocity at the vena contracta

μ : Kinematic viscosity
U_{DK} : Drift velocity

References

[1]. J. Speerli and W. H. Hager, (2000),"Air-water flow in bottom outlets", Can. J. of Civ. Eng. Vol. 27, No.3.

[2]. R. B. Eddington, (1970), "Investigation of supersonic phenomena in a two-phase (liquid-gas) tunnel". AIAA J, Vol. 8, pp 65–74.

[3]. H. Falvay, (1980), "Air-water flow in hydraulic structure", US department of interior, Water and power resources service, Denver, Colorado, Engineering monograph, No. 41.

[4]. H. Chanson, T. Brattberg, (2000), "Experimental study of the air-water shear flow in a hydraulic jump", International J. of multiphase flow, Vol.28, pp. 583-607.

[5]. L. Toombes and H.Chanson, (2005), "Air Entrainment and velocity redistribution in a bottom outlet jet flow", XXXI IAHR Congress 2717, Seoul, Korea.

[6]. W. Somchai and W. Kalinitchenko, (2002), "Mean velocity distribution in horizontal Air-water flow", International J. of multiphase flow Vol. 28, pp. 167-174.

[7]. E. Naudascher, (1986), "Prediction and control of downpull on tunnel gates", J. Hydraulic Eng, ASCE, Vol 112,No 5.

[8]. I. Aidin, (2002),"Air demand behind of

high head gates during emergency closure" J. of hydraulic research, ASCE, Vol. 40, No. 1.

[9]. US army corps of engineers, (1988), "Air-demand design criteria", Engineering manual, EM-1110-2-1602.

[10]. W. H. XIA (1997),"Modeling similitude of high speed aerated flow", J. Hydrodynamics, Vol. 47, No. 55.

[11]. B. T. Sagar A. and Tullis J. P, (1979), "Downpull on vertical lift gates", Water power & dam construction.

[12]. J. F. Zhao, (1998), "Study on the compressibility of aerated water flow". PHD dissertation, Wuhan university of hydraulic & electric engineering, Wuhan, P. R. China (in Chinese).

[13]. H. Chanson, (1996), "Air bubble entrainment in free surface turbulent shear flows", Academic press, San Diago.

[14]. H. R. Sharma, (1976), "Air entrainment in high head gated conduits", J. Hydarulics division, ASCE, Vol. 102, No. 11.

[15]. E. Naudascher, (1991), "Hydrodynamic Forces", A. A. Balkema, Rotterdam.

[16]. C. S. Lauchlan and M. Escarameia, R. W. P. May, R. Burrows, (2005), "Air in pipelines", Literature review, Report SR.649, Rew.2, HR Wallingford.

[17]. JH. Ferziger and M. Peric, (1997), "Computational methods for fluid dynamics",Berlin springer,(Chapter 7).

[18]. Fluent team, (2000). "Manual and User guide of Fluent software",Fluent Inc. Centerra Resource Park 10 Cavendish Court Lebanon, NH 03766

[19]. TJ. Craft, BE. Launder, K. Suga, (1996), "Development and application of a cubic eddy viscosity model of turbulence", Int J. Heat fluid flow, Vol.17, No.15.

[20]. F. Durst and F. Schmitt, (1985), "Experimental studies of high-Reynolds number backward-facing step flows", Proc. 5 th Symp. Turbulent shear flows, Cornell Univ.

[21]. Fluent team, (2000). "Manual and User guide of Gambit software",Fluent Inc. Centerra Resource Park 10 Cavendish Court Lebanon, NH 03766

[22]. C.V. Davis and K. E .Sorenson,(1984), "Hand book of applied hydraulics", Third edition, McGraw hill book company, Tokyo.

[23]. Jose G.Vasconcelos,(2000),"Numerical Modeling of the Transition Between Free Surface and Pressurized Flow in Storm Sewers", University of Michigan Environmental and Water Resources Engineering, 49109-2125, Ann Arbor, USA.

[24]. Trajkovic, B., Ivetic, M., Calomino, F., D'Ippolito, A., (1999). "Investigation of transition from free surface to pressurized flow in a circular pipe", Water Science and Technology, 39 (9), 105-112.